ChemComm

Thermally robust solvent-free biofluids of M13 bacteriophage engineered for high compatibility with anhydrous ionic liquids

Journal:	*ChemComm*
Manuscript ID	CC-COM-06-2019-004909.R1
Article Type:	Communication

COMMUNICATION

Thermally robust solvent-free biofluids of M13 bacteriophage engineered for high compatibility with anhydrous ionic liquids

Received 00th January 20xx,
Accepted 00th January 20xx

DOI: 10.1039/x0xx00000x

Alex P. S. Brogan[a,b†], Nimrod Heldman[c,d†], Jason P. Hallett[a*], Angela M. Belcher[c,d,e*].

Here, we demonstrate a chemical modification strategy to create biomaterials of the M13 bacteriophage with extraordinary thermal stability, and high compatibility with non-aqueous ionic liquids. The results provide a blueprint for developing soft materials with well-defined architectures that may find broad applicability in the next generation of flexible devices.

Soft materials, gels and polymer-melts, are increasing in popularity, most notably in the emerging fields of bioelectronics[1], soft robotics[2], and wearable sensors[3]. As these fields develop, the requirements for increasing complexity within these systems introduces challenges in maintaining their attractive properties. The lack of order within soft materials – essential for flexibility – is a significant hurdle to the introduction of complexity. Utilization of biomolecules – proteins, viruses, and DNA – can provide local hierarchical order (nanoscale structure) without impacting global disorder (macroscale structure). Ionic liquids, organic salts with melting points typically below 100 °C, are a relatively new class of solvent with a range of tuneable and desirable properties such as negligible vapour pressure, ionic conductivity, and broad chemical and thermal stabilities. Despite the powerful combination of programable scaffolds and unique solvent capabilities, to date, there are no examples of soft materials comprising of functional biomolecules and ionic liquids. Such materials could have advantageous properties for interfacing biology with artificial systems.

[a.] *Department of Chemical Engineering, Imperial College London, London, SW7 2AZ, UK.*
[b.] *Department of Chemistry, King's College London, Britannia House, London, SE1 1DB.*
[c.] *Department of Biological Engineering, Massachusetts Institute of Technology, 77 Massachusetts Avenue, 76-561, Cambridge, USA.*
[d.] *Koch Institute for Integrative Cancer Research, Massachusetts Institute of Technology, 77 Massachusetts Avenue, 76-561, Cambridge, USA.*
[e.] *Department of Materials Science and Engineering, Massachusetts Institute of Technology, 77 Massachusetts Avenue, 76-561, Cambridge, USA.*
†Authors contributed equally
Electronic Supplementary Information (ESI) available: Experimental details, additional thermal analysis, additional SAXS analysis, and additional SRCD analysis. See DOI: 10.1039/x0xx00000x

Solvent-free biofluids are a new class of material where surface modification of proteins allows for a liquid phase in the absence of solvent.[4–8] These have been shown to preserve biomolecule structure[5,8,9] and enzymatic function[7] in the absence of water, and importantly, significantly enhance thermal stability.[4] Recently, we demonstrated that this biotechnology can be used to solubilize and stabilize proteins in ionic liquids.[10,11]

M13 is a filamentous bacteriophage with an extraordinary aspect ratio, with a length of *ca*. 900 nm and width of *ca*. 6 nm. Furthermore, it has been used as a versatile, and genetically engineerable, template for a number of nanomaterial assemblies.[12–14] As a result, it is an ideal archetypal building block for future bio-based devices that sit at the interface of materials and biology. Here, we demonstrate for the first time a thermally robust biofluid of the M13 bacteriophage that has retained structural integrity and high compatibility with anhydrous ionic liquids.

Solvent-free biofluids of M13 filamentous bacteriophage ([C-M13][S]) were prepared using established methods optimised for the larger dimensions of the bacteriophage construct (see Supplementary Information)[10,15,16]. Nanoconjugates of M13 and S_1 and S_2 were formed by electrostatic complexation to C-M13 to yield [C-M13][S_1] and [C-M13][S_2], which had surfactant:p8 coat protein ratios of 19:1 (Fig. 1a). Synchrotron radiation circular dichroism (SRCD) spectroscopy (Fig. 1b) was deconvoluted to show that the α-helicity of the p8 coat protein increased from 25 % to 49 % upon formation of the nanoconjugate (Fig. 1b, SI Table 1). Remarkably, dynamic light scattering measurements (Fig. 1c) indicated that this increase in secondary structure did not relate to a change in the overall quaternary structure of the virus, an observation confirmed by the presence of filamentous structure by transmission electron microscopy (TEM, Fig. 1d).

Solvent-free biofluids of [C-M13][S] were obtained by freezedrying the nanoconjugates to remove all water, followed

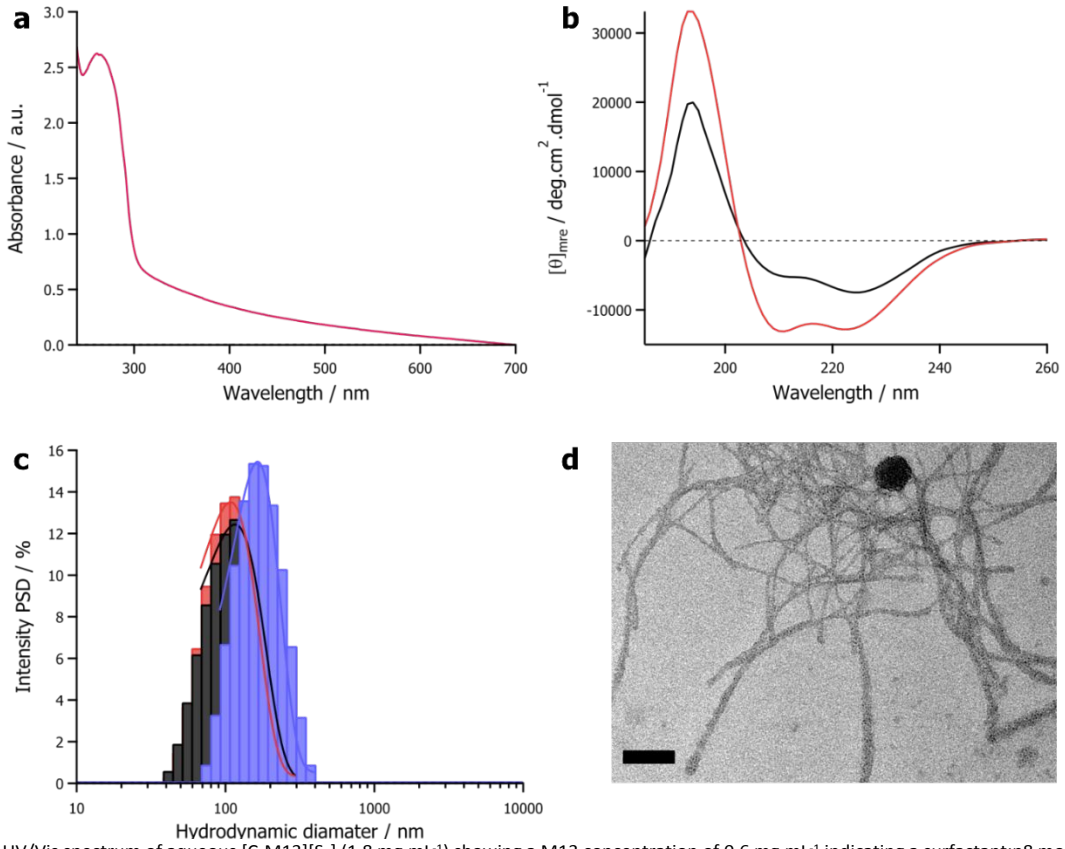

Figure 1. (**a**) UV/Vis spectrum of aqueous [C-M13][S_2] (1.8 mg.mL^{-1}) showing a M13 concentration of 0.6 mg.mL^{-1} indicating a surfactant:p8 molecular ratio of 19:1. M13 spectrum (0.6 mg.mL^{-1}, black) is provided for reference. (**b**) SRCD spectra of aqueous M13 (black) and [C-M13][S_2] (red). (**c**) Plot of particle size distribution by intensity against hydrodynamic diameter (measured by DLS) for aqueous M13 (black), C-M13 (red), and [C-M13][S_2] (blue). Distributions fitted with Gaussian plots. (**d**) Transmission electron micrograph of [C-M13] showing maintained bacteriophage supramolecular structure (scale bar = 100 nm).

by annealing at 80 °C to form off-white homogenous waxy liquid-like materials. Differential scanning calorimetry (DSC) measurements (Fig. 2a) showed thermal transitions for both [C-M13][S_1] and [C-M13][S_2] that were distinctly different from those of the pure surfactant (SI Fig. 1), indicating that the obtained biofluids were pure liquid phases of M13. Both [C-M13][S_1] and [C-M13][S_2] displayed similar thermal transitions, most notably being the presence of a second melting transition at 58 °C (Fig. 2a). This was most prominent for [C-M13][S_2], and suggested that there were 3 distinct phases. The first – a transition between solid and a liquid crystal phase occurring at 27 °C, followed by a second – a transition between a liquid crystal phase and an isotropic fluid phase at 58 °C. Temperature dependent wide angle X-ray scattering (WAXS) was used to probe the surfactant corona around the bacteriophage in response to the different phases. Profiles for [C-M13][S_2] (Fig. 2c) showed distinct peaks at 1.34 Å^{-1} and 1.61 Å^{-1}, corresponding to separations of 4.7 Å and 3.9 Å respectively. These were consistent with PEG-PEG and alkyl-alkyl chain interactions between surfactant molecules in the solvent-free biofluid. These peaks persist between 0 and 50 °C, albeit with diminishing intensity, indicating increasing disorder within the system going from the solid phase to the liquid crystal phase. Above 60 °C however, these peaks are completely absent, replaced by a single broad feature at 1.37 Å^{-1} (4.6 Å), indicating the absence of any crystallinity. Attenuated total reflection (ATR) FTIR was used to confirm retention of α-helical structure of the phage in the solvent-free biofluid (Fig. 2b). Amide I and II peaks at 1655 cm^{-1} and 1545 cm^{-1} respectively confirmed this was the case for both [C-M13][S_1] and [C-M13][S_2].

Our previous studies on solvent-free biofluids of small proteins and enzymes has shown that they had both high thermal stability, and good compatibility with ionic liquids. Here, we set out to demonstrate that this was also possible for biofluids of significantly larger biological constructs (μm *vs.* nm). SRCD of [C-M13][S_2] in the solvent-free fluid and when dispersed in (UV clear) ionic liquids (Fig. 3a) showed spectra that was consistent with significant α-helical structure, indicating that secondary structure was maintained under these anhydrous conditions (Fig. 3a, SI Table 1). Specifically, spectra deconvolution estimated α-helicity at 42 % in solvent-free state, 39 % in [bmpyrr][OTf], 40 % in [bmpyrr][$MeSO_4$], and 44% in [bmpyrr][NTf_2]. These values were broadly in line with that of [C-M13][S_2] in aqueous solutions (49 %).

Small angle X-ray scattering (SAXS) was used to investigate the quaternary architecture of the virus in the solvent-free biofluid and ionic liquids. SAXS plots for [C-M13][S_2] in the solvent-free state, and in [bmpyrr][OTf], [bmpyrr][$MeSO_4$], and [bmpyrr][NTf_2] all showed features at 0.082 Å^{-1} and 0.15 Å^{-1}, corresponding to separation distances of 80.0 Å and 41.7 Å respectively. These distances were consistent with centre-centre correlations between neighbouring phage molecules in concentrated liquids, and the internal diameter of the phage. Crucially, the persistence of the internal phage diameter (*ca*. 4

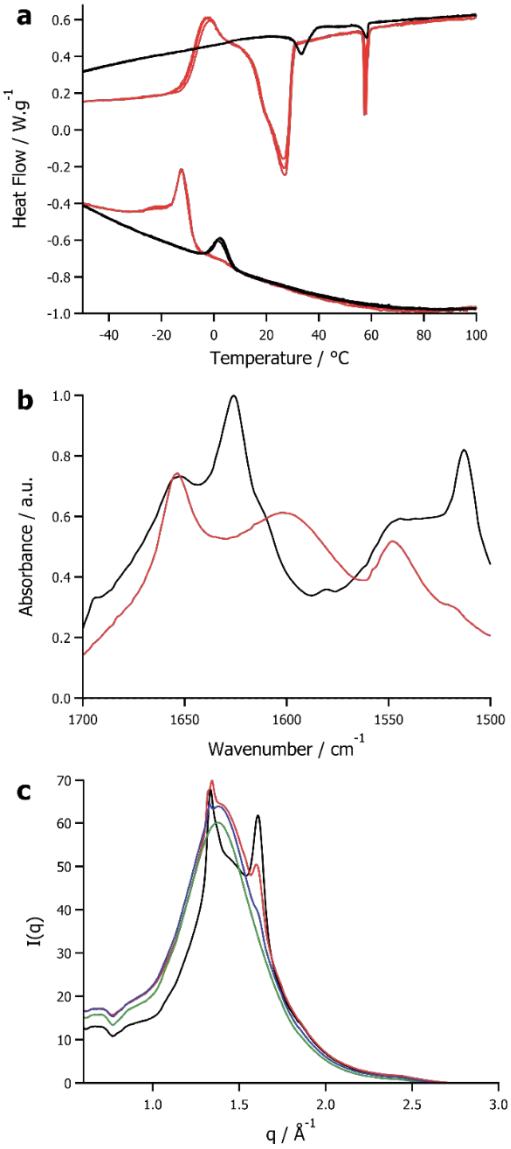

Figure 2. (**a**) DSC thermogram showing heating and cooling cycles of [C-M13][S_1] (black) and [C-M13][S_2] (red). First cycles were discarded to account for thermal history of the samples. (**b**) ATR-FTIR spectrum showing amide I/II region for [C-M13][S_1] (black), and [C-M13][S_2] (red). (**c**) WAXS profiles for [C-M13][S_2] recorded at 0 °C (black), 30 °C (red), 50 °C (blue), and 60 °C (green).

nm) indicated that global phage structure was maintained in the solvent-free biofluid, and in ionic liquids (Fig. 3b). Temperature dependent SAXS was used to investigate the thermal stability of the modified phage in solvent-free biofluids (Fig. 3c) and ionic liquids (SI Fig. 2). Increasing the temperature from 0 °C to 90 °C had no significant impact on the dimensional features observed in the SAXS plots for solvent-free liquid [C-M13][S_2] (Fig. 3c,d). At temperatures above 90 °C, the feature at low q (0.082 $Å^{-1}$) broadens and shifts to lower q at 150 °C (0.044 $Å^{-1}$), indicating an increase in the phage-phage separation in the biofluid from 80.0 Å to 143.9 Å, consistent with increased disorder within the biofluid at higher temperatures. The feature at higher q (0.15 $Å^{-1}$) attributed to the internal diameter of the phage (41.7 Å), however, remained constant up to 160 °C (Fig. 3c,d). This indicated that macromolecular architecture of solvent-free liquid phage was incredibly thermally robust, an important feature for future applications.

Temperature dependent SRCD (SI Fig. 3a) confirmed high thermal stability of the solvent-free phage biofluid with respect to secondary structure. Using a two-state model of denaturation, a plot of fraction denatured (SI Fig. 3b) indicated a half denaturation temperature (T_m) of 184 °C. This was an increase in thermal stability of almost 100 °C compared to the aqueous nanoconjugate (86 °C, SI Fig. 4). In broad agreement with the SAXS data, the folded state of solvent-free [C-M13][S_2] was maintained up to 150 °C, with denaturation occurring as the temperature increased further. This demonstrated that the loss of the internal diameter of the phage was concomitant with a loss in secondary structure. As such, it was clear that both secondary, tertiary, and quaternary structure of the M13 bacteriophage had been maintained and significantly enhanced in the absence of solvent.

Given the high thermal stability of the phage biofuid, and the maintained structure of [C-M13][S_2] in ionic liquids (Fig. 3a,b), temperature dependent SAXS profiles (SI Fig. 2) were used to assess thermal stability of [C-M13][S_2] in ionic liquids. Similarly to the solvent-free case, thermal robustness of [C-M13][S_2] was also evident when dispersed in ionic liquids. Specifically, the phage internal diameter remained a constant 41 – 45 Å in [bmpyrr][$MeSO_4$], [bmpyrr][OTf], and [bmpyrr][NTf_2] up to 150 °C, 200 °C, and 170 °C respectively (SI Fig. 2). Comparable to what was observed in the solvent-free biofluid, this showed that the architecture of the M13 bacteriophage could not only be maintained in the non-aqueous environments, but at high temperatures also. This demonstrated further the applicability of phage biofluids, where thermal robustness was translated in both hydrophilic and hydrophobic ionic liquids. As such, solvent-free biofluids have rich potential in delivering and stabilizing filamentous bacteriophage to anhydrous ionic liquid media. The maintained structural fidelity of the virus in the absence of water and at high temperatures, demonstrates how genetically programmable functional scaffolds may be incorporated into future advanced soft materials.

In conclusion, we have shown for the first time, that chemical modification of the M13 bacteriophage can yield a solvent-free

biofluid that is compatible with both hydrophilic and hydrophobic ionic liquids. The secondary and quaternary structure of the phage was maintained in the anhydrous environments as evidenced by SRCD, SAXS and TEM. Significantly, thermal stability was greatly enhanced compared to aqueous solutions, with phage structure persisting in the solvent-free liquid and ionic liquids up to 150 °C. As a result, we demonstrate a new biomaterial for introducing M13 bacteriophage as a high aspect ratio, genetically encodable, and chemically functionalizable building block in non-aqueous environments. Where retained quaternary structure of the virus provides a highly organised scaffold within an ionic liquid environment. Therefore, these results provide the basis for the creation of a new class of soft materials with well-defined nanoscale architectures, high thermal robustness, and expanded versatility with respect to material environment.

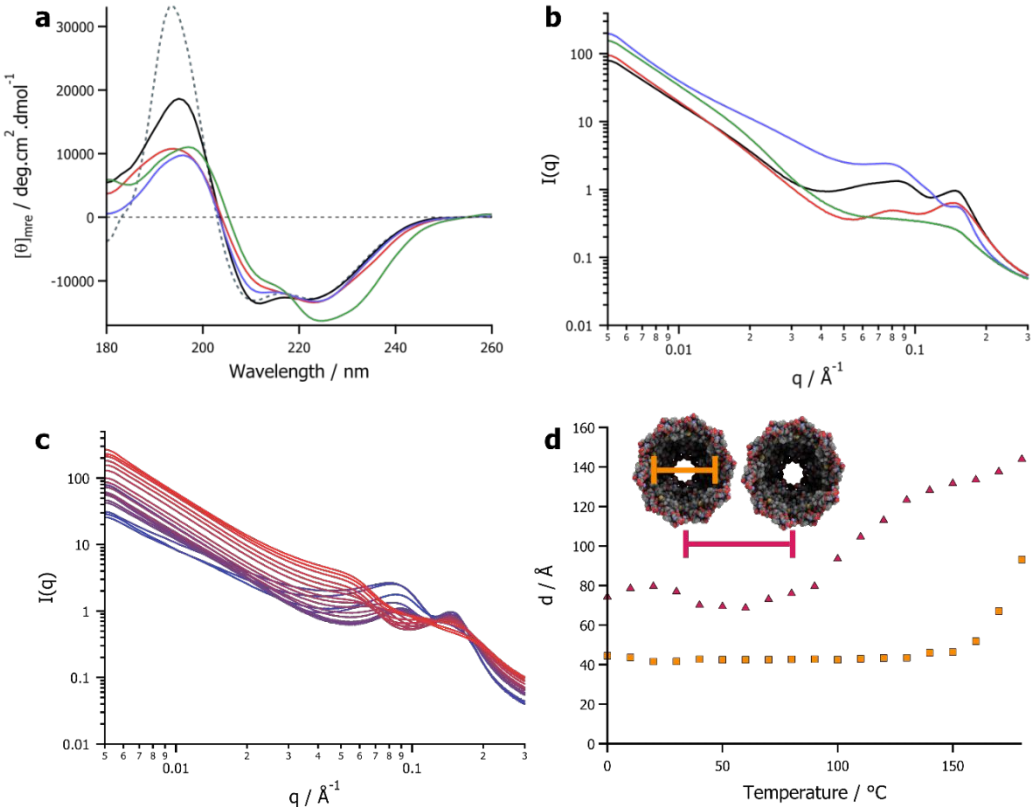

Figure 3. (**a**) SRCD spectra of [C-M13][S_2] solvent-free biofluid (black), and dissolved in [bmpyrr][OTf] (red), [bmpyrr][$MeSO_4$] (blue), [bmpyrr][NTf_2] (green), and water (dashed grey). (**b**) SAXS plots for [C-M13][S_2] in solvent-free biofluid (black), [bmpyrr][OTf] (red), [bmpyrr][$MeSO_4$] (blue), and [bmpyrr][NTf_2] (green). (**c**) Temperature dependent SAXS plots for solvent-free [C-M13][S_2] from 0 °C (blue) to 180 °C (red). (**d**) Plot of distance against temperature for internal diameter (yellow) and phage separation (purple) [depicted in graphical inset] against temperature for solvent-free [C-M13][S_2] as calculated from corresponding SAXS plot.

Acknowledgements

The authors would like to thank The MIT-Imperial College London MISTI Global Seed Fund, the U.S. Defense Advanced Research Projects Agency's Living Foundries program award HR0011-15-C-0084, and the EPSRC (Frontier Engineering Grant EP/K038648/1) for providing funding for this work. The authors also thank Prof. G. Siligardi, Dr. R. Hussain and Dr. T. Jaforvi at the Diamond Light Source for access to the B23 beamline, Dr. N. Terrill and Dr. A. Smith at the Diamond Light Source for access and support at the I22 beamline.

Conflicts of interest

There are no conflicts to declare.

Notes and references

1 T. Someya, Z. Bao and G. G. Malliaras, *Nature*, 2016, **540**, 379–385.

2 G. M. Whitesides, *Angew. Chem. Int. Ed.*, 2018, **57**, 2–18.

3 Y. Liu, K. He, G. Chen, R. Leow and X. Chen, *Chem. Rev.*, 2017, **117**, 12893–12941.

4 A. P. S. Brogan, G. Siligardi, R. Hussain, A. W. Perriman and S. Mann, *Chem. Sci.*, 2012, **3**, 1839–1846.

5 F.-X. Gallat, A. P. S. Brogan, Y. Fichou, N. McGrath, M. Moulin, M. Härtlein, J. Combet, J. Wuttke, S. Mann, G. Zaccai, C. J. Jackson, A. W. Perriman and M. Weik, *J. Am. Chem. Soc.*, 2012, **132**, 13168–13171.

6 A. P. S. Brogan, R. B. Sessions, A. W. Perriman and S. Mann, *J. Am. Chem. Soc.*, 2014, **136**, 16824–16831.

7 A. P. S. Brogan, K. P. Sharma, A. W. Perriman and S. Mann, *Nat. Commun.*, 2014, **5**, 5058.

8 A. W. Perriman, A. P. S. Brogan, H. Cölfen, N. Tsoureas, G. R. Owen and S. Mann, *Nat. Chem.*, 2010, **2**, 622–626.

9 A. P. S. Brogan, K. P. Sharma, A. W. Perriman and S. Mann, *J. Phys. Chem. B.*, 2013, **117**, 8400–7.

10 A. P. S. Brogan and J. P. Hallett, *J. Am. Chem. Soc.*, 2016, **138**, 4494–4501.

11 A. P. S. Brogan, L. Bui-Le and J. P. Hallett, *Nat. Chem.*, 2018, **10**, 859–865.
12 Y. J. Lee, H. Yi, W.-J. Kim, K. Kang, D. S. Yun, M. S. Strano, G. Ceder and A. M. Belcher, *Science*, 2009, **324**, 1051–1055.
13 C. Mao, D. J. Solis, B. D. Reiss, S. T. Kottmann, R. Y. Sweeney, A. Hayhurst, G. Georgiou, B. Iverson and A. M. Belcher, *Science*, 2004, **303**, 213–217.
14 S. M. Jung, J. Qi, D. Oh, A. Belcher and J. Kong, *Adv. Funct. Mater.*, 2017, **27**, 1603203.
15 H. Park, N. Heldman, P. Rebentrost, L. Abbondanza, A. Iagatti, A. Alessi, B. Patrizi, M. Salvalaggio, L. Bussotti, M. Mohseni, F. Caruso, H. C. Johnsen, R. Fusco, P. Foggi, P. F. Scudo, S. Lloyd and A. M. Belcher, *Nat. Mater.*, 2015, **15**, 211–216.
16 C. F. I. Barbas, D. R. Burton, J. K. Scott and G. J. Silverman, *Phage display: A laboratory manual*, Cold Spring Harbor Laboratoty Press, New York, 2001.